Active phase drift cancellation for optic-fiber frequency transfer using a photonic radio-frequency phase shifter

Jianguo Shen,[1,2] Guiling Wu,[1,*] Liang Hu,[1] Weiwen Zou,[1] and Jianping Chen[1]

[1]*State Key Laboratory of Advanced Optical Communication Systems and Networks, Department of Electronic Engineering, Shanghai Jiao Tong University, Shanghai 200240, China*

[2]*College of Mathematics, Physics and Information Engineering, Zhejiang Normal University, Jinhua 321004, China*

**Corresponding author: wuguiling@sjtu.edu.cn*

Received January 31, 2014; accepted February 28, 2014;
posted March 17, 2014 (Doc. ID 205854); published April 9, 2014

We propose an active photonic phase drift cancellation scheme for frequency transfer over optical fiber based on a linear photonic RF phase shifter. The photonic RF phase shifter consists of a dual parallel Mach–Zehnder modulator and optical filter with the assistance of the local microwave signal. The phase drift induced by fiber transmission can be compensated by simply tuning the bias voltage of the modulator. The principle of the phase cancellation scheme based on the photonic phase shifter is demonstrated and validated experimentally by transferring a 0.5 GHz reference signal over a 20 km single-mode fiber with a root mean square jitter of less than 0.5 ps.

OCIS codes: (060.2360) Fiber optics links and subsystems; (060.5625) Radio frequency photonics; (120.3940) Metrology.

http://dx.doi.org/10.1364/OL.39.002346

Ultrastable frequency remote transfer plays a key role in many applications such as very long baseline interferometers, clock comparison, and physical constant measurement [1]. Due to the advantages of low loss, high reliability, and wide bandwidth, optical fiber link is considered to be a promising option for frequency reference remote transfer and has attracted an intensive research interest in recent years [2–8]. One of the key issues to realize stable frequency transfer via optical fiber is to cancel the phase drift induced by the temperature variation and mechanical perturbation along optical fiber transmission.

To date, several phase drift cancellation schemes in the optical domain or electrical domain have been proposed. The phase drift cancellation based on a tunable optical true delay line composed of a piezoelectric fiber stretcher and a temperature-controlled fiber spool has been adopted and demonstrated on field optical fiber links by several groups [2,3]. Although such a scheme can achieve a high suppression ratio of phase drift and support a large RF bandwidth, a temperature-controlled optical delay line with a large dynamic range is considerably bulky and has high power consumption. Moreover, the piezoelectric fiber stretcher will also induce an additional polarization mode dispersion and amplitude noise. Recently, a phase drift cancellation scheme based on a λ dispersion optical tunable delay has been reported [4]. In this scheme, the whole fiber link is used as part of the tunable device, and the tunable delay range is in proportion to the length of the fiber link. However, a broadband tunable laser with a high wavelength tuning precision is needed to realize high-precision and large dynamic phase compensation. And its delay tuning precision decreases with the increase of the length of the fiber link. Similar to the optical domain techniques, tunable electrical phase shift devices such as voltage control oscillators (VCOs) [5,6] and phase shifters [7,8], can also be used to compensate the phase drift of frequency transfer by the phase conjugation method [9]. The VCO has a large tuning range and fast tuning speed. It, however, has a band-limited frequency range [4]. The electrical phase shifters suffer from a variable insertion loss which will result in an excess amplitude-to-phase noise conversion.

In this Letter, we propose a novel phase drift cancellation scheme for frequency transfer over optical fiber using a linear photonic RF phase shifter as a phase compensator. The photonic phase shifter consists of a dual parallel Mach–Zehnder modulator (DPMZM) and optical filter with the assistance of the local microwave signal, which has a linear phase shift of more than 360 deg and a low power variation of less than 0.3 dB [10]. The phase drift induced by fiber transmission is cancelled by simply controlling one of the bias voltages of the DPMZM according to the phase error signal. Moreover, the photonic phase shifter also acts as a single sideband transmitter, which not only makes the system simpler but also can overcome the chromatic-dispersion-induced RF power fading in long-distance fiber transmission, especially for higher frequencies [11]. The proposed phase cancellation scheme is demonstrated experimentally by transferring a 0.5 GHz frequency reference signal over a 20 km single-mode fiber with a root mean square jitter of less than 0.5 ps.

Figure 1 illustrates the proposed phase drift cancellation scheme based on a photonic RF phase shifter schematically. The photonic RF phase shifter is shown in the dashed block, which is composed of a laser, DPMZM, and optical bandpass filter (OBPF) with the assistance of the local microwave signal and electric upconverter (U-C). An erbium-doped fiber amplifier (EDFA) is adopted to compensate the insertion loss of the DPMZM and OBPF. The bias voltages of the two sub-MZMs are biased at the minimum transmission point to perform optical carrier suppressed double sideband (CPS-DSB) modulation. Assuming that the two lower sidebands of the CPS-DSB

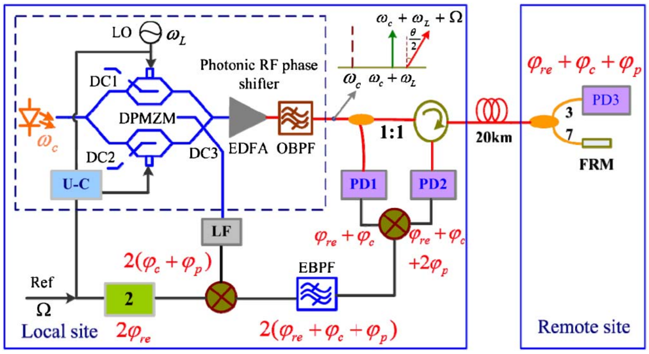

Fig. 1. Schematic of the phase drift cancellation based on photonic RF phase shifter. DPMZM, dual parallel Mach–Zehnder modulator; PC, polarization controller; EDFA, erbium-doped fiber amplifier; OBPF, optical bandpass filter; PD, photodetector; FRM, Farad rotation mirror; EBPF, electrical bandpass filter; U-C, upconverter; LF, loop filter.

signals are suppressed by the OBPF, a phase tunable single sideband signal obtained at the output of the photonic RF phase shifter can be expressed as follows:

$$E_A(t) \propto A_2 \exp\left[j\left(\omega_c t + (\omega_L + \omega_r)t + \varphi_{re} + \frac{\varphi_c}{2}\right)\right] + A_1 \exp\left[j\left(\omega_c t + \omega_L t - \frac{\varphi_c}{2}\right)\right], \tag{1}$$

where A_1 and A_2 are the amplitude of the first-order sideband on the top and bottom arm, respectively; ω_c, ω_L, and ω_r are the frequency of the optical carrier, local microwave, and frequency reference signals, respectively; φ_{re} is the initial phase of the reference frequency signal, $\varphi_c = \pi V_3/V_{\pi 3}$ is the phase difference between the optical modulation sidebands on the top and bottom arm, $V_{\pi 3}$ is the half-wave voltage of the parent MZM, and V_3 is the bias voltage of the parent MZM (DC3).

The modulated optical signal from the photonic RF phase shifter is divided into two parts. One part is detected by the PD1 to generate a phase-shifted frequency reference signal, which can be given by

$$V_1 \propto \cos(\omega_r t + \varphi_c + \varphi_{re}). \tag{2}$$

The other part is transmitted to a remote site through an optical fiber link. At the remote site, the modulated light is detected by the PD3 to obtain the delivered reference frequency signal, which can be express as

$$V_3 \propto \cos(\omega_r t + \varphi_c + \varphi_{re} + \varphi_p), \tag{3}$$

where φ_p is the phase induced by the fiber transmission. At the same time, this received reference frequency signal is returned to the local site through the same optical fiber link by reflecting part of the received modulated light or a regeneration approach. The round-trip signal is detected by the PD2 at the local site. Assuming that optical signal transfer over the same fiber in both directions experiences the same phase fluctuation, the round-trip signal can be expressed as

$$V_2 \propto \cos(\omega_r t + \varphi_c + \varphi_{re} + 2\varphi_p). \tag{4}$$

The signals V_1 and V_2 are mixed and filtered by an electrical bandpass filter (EBPF) with the central frequency of $2\omega_r$ to obtain the sum-frequency signal $\cos(2\omega_r t + 2\varphi_{re} + 2\varphi_c + 2\varphi_p)$. Then a phase detector is used to acquire the phase difference φ_{error} between this sum-frequency signal and the frequency-doubling reference signal $\cos(2\omega_r t + 2\varphi_{re})$ generated by a frequency multiplier:

$$\varphi_{\text{error}} = 2(\varphi_c + \varphi_p). \tag{5}$$

This phase difference after processed by a loop filter is used to tune the φ_c by controlling the bias voltage DC3 to compensate the phase drift of φ_p. When the control loop works properly, the φ_{error} equals zero ($\varphi_c = -\varphi_p$). Thus, the phase of the recovered reference signal at the remote site is φ_{re}, and fiber-induced phase fluctuation is cancelled. A copy of the frequency reference signal is obtained at the remote user.

To verify the principle of the proposed phase drift cancellation scheme, a 20 km frequency transfer experimental system based on the setup in Fig. 1 is built. The optical carrier from a tunable laser (Alnair, TLG-200) with a linewidth of less than 100 kHz is injected into a DPMZM (Photline, MXIQ-LN-40) with a bandwidth of 20 GHz and insertion loss of 5 dB. The frequency of the reference signal is 0.5 GHz, and the frequency of the local microwave signal is set at 10 GHz to ensure that the two lower sidebands can be suppressed completely by the consequent tunable optical bandpass filter (TOBPF, Alnair, BLV-200CL). The central frequency and bandwidth of the TOBPF are adjusted to satisfy Eq. (1). At the remote end, 30% of the received optical power coupled out by a 30:70 optical coupler is injected into the PD3 while the other part is reflected by a Faraday rotation mirror (FRM).

Figure 2(a) shows the optical spectrum at the output of the photonic phase shifter measured by a high-resolution optical spectral analyzer (Apex, AP2040A). We can see that two lower sidebands are suppressed by more than 46 dB compared with the two upper sidebands. Hence, its influence on the performance of the phase shifter can be ignored [12]. The residual optical carrier mainly comes from the finite extinction ratio of the DPMZM (about 20 dB), but it has no effect on the recovered reference signal since the beat signals between the optical carrier and the two upper sidebands can be removed by the EBPF after photodetectors (PDs). In this case, the photonic phase shifter can be regarded as a single sideband transmitter. In order to achieve an optimal SNR, the powers of the two upper sidebands are set to be equal by controlling the RF powers applied on two sub-MZMs [13]. The characteristics of the phase shift are shown in Fig. 2(b). A continuous and linear phase shift of more than 450 deg and power variation of less than 0.3 dB are achieved when the bias voltage (V_3) is tuned from −18 to 18 V. The measured phase tuning bandwidth of the phase shifter is more than 10 MHz. The tuning bandwidth is sufficient for the round-trip phase cancellation scheme since the loop bandwidth limited by the

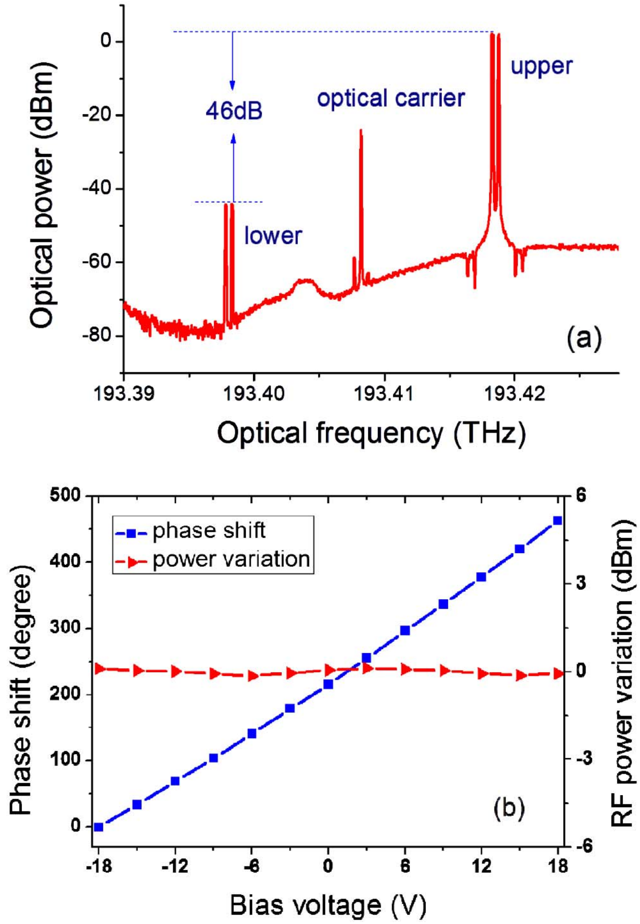

Fig. 2. Performance of the photonic phase shifter: (a) optical spectrum at the output of the OBPF and (b) measured phase shift and power variation as the bias voltage tuning.

round-trip delay is less than 2 kHz for the frequency transfer over more than 10 km optical fiber [1].

Figure 3 shows the timing jitter of the received frequency reference signal without and with the phase compensation based on the above photonic phase shifter. As can be seen, the timing drift (slow drift) without compensation is up to 180 ps within 10,000 s, which is mainly caused by the ambient temperature change. With the compensation based on the proposed scheme, the root mean square timing jitter can be suppressed to less than 0.5 ps. A slight delay drift of about 2 ps can still be observed. The main reasons are as follows: (i) the transmission delay fluctuations of the fibers, cables, and phase detectors out of the control loop with the temperature change; and (ii) the accuracy of measured phase error is degraded by the excess parasitic phase noises, which are induced by the second harmonic and the intermodulation components with the frequency of $2\omega_r$ originating from the nonlinearity of the mixer. In practice, Eq. (5) should be modified as $\varphi_{\text{error}} = 2[\varphi_c + (1+k)\varphi_p]$, where $k\varphi_p$ represents the excess parasitic phase and k is a coefficient related to the nonlinearity of the mixer. When the φ_{error} equals zero, the excess phase $k\varphi_p$ will remain in the recovered reference signal at the remote site, and the suppression ratio of the phase drift will be limited by the value of k. An additional temperature control and a better mixer with a low second harmonic and the four-order intermodulation components can be used to improve the compensation precision [14].

Figure 4 shows the phase noise spectrum density of the optical link measured by a phase noise analyzer (PN9000). We can see that the phase noise near the carrier (fast fluctuation) is effectively suppressed when the phase compensation is activated. However, the phase noise suppression ratio at higher frequencies in the control bandwidth about 50 Hz is limited, which is mainly attributed to the poor noise floor of the phase detector and loop filter. The phase noise out of the control bandwidth is dominated by the amplified spontaneous emission (ASE) noise of the EDFA since the input optical power to the EDFA is less than −17 dBm. A laser source with a high optical power can be used to improve the EDFA's ASE noise.

It is worthwhile to mention that the phase drift of the adopted photonic phase shifter itself can also be detected and compensated and has a negligible impaction on the compensation precision in our scheme. This is because the photonic phase shifter is in the phase control loop, and the phase drift of the photonic phase shifter is less than 0.5 deg within 2000 s in an open experimental

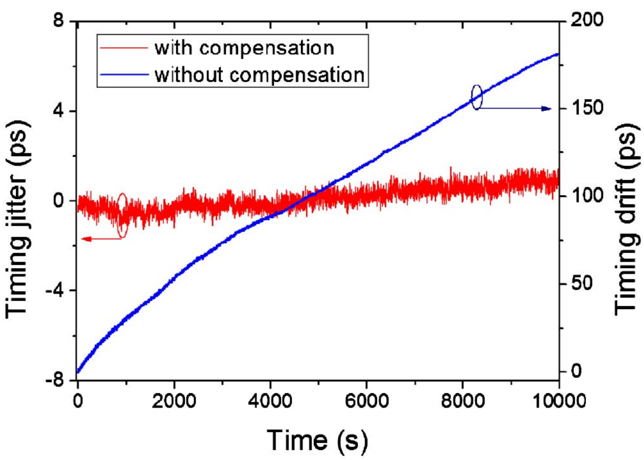

Fig. 3. Timing jitters of 20 km optical link with and without phase compensation.

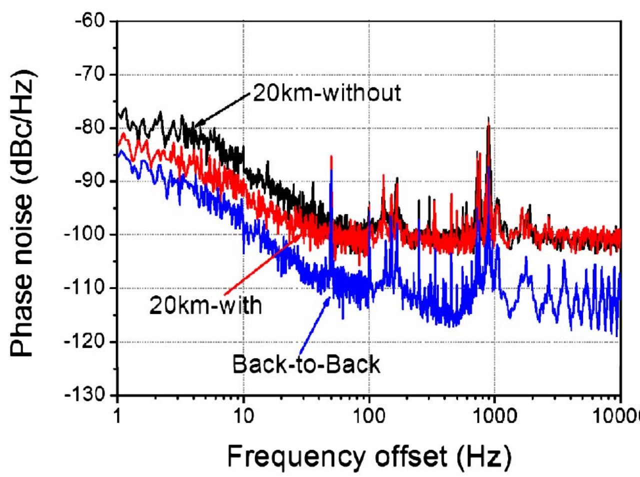

Fig. 4. Phase noise spectrum of back-to-back link (blue) and 20 km link with compensation (red) and without compensation (black).

condition [10], which is far less than the phase drift induced by the fiber link.

In conclusion, we proposed and experimentally demonstrated a photonic RF phase-shifter-based phase drift cancellation scheme for frequency transfer over optical fiber, where the phase drifts induced by fiber transmission can be suppressed by simply controlling the bias voltage of the modulator. The proposed scheme is validated experimentally by transferring a 0.5 GHz reference signal over a 20 km single-mode fiber with a root mean square jitter of less than 0.5 ps. Actually, the highest frequency of the transferred reference signal can be up to 10 GHz in our system, which is mainly limited by the bandwidth of the DPMZM. We plan to optimize the resolution of phase detection and suppress the excessive parasitic phase noise induced by the mixer to improve compensation precision in future work.

This work was supported in part by the 973 Program (2011CB301700), the National Natural Science Foundation of China (61071011, 61127016, and 61007052), the Shanghai Excellent Academic Leader Program (Grant No. 12XD1406400), SRFDP of MOE (Grant No. 20130073130005), and the Zhejiang Provincial Nature Science Foundation of China (LY12F05002).

References

1. S. M. Forma, K. W. Holman, D. D. Hudson, D. J. Jones, and J. Ye, Rev. Sci. Instrum. **78**, 021101 (2007).
2. G. Marra, R. Slavík, H. S. Margolis, S. N. Lea, P. Petropoulos, D. J. Richardson, and P. Gill, Opt. Lett. **36**, 511 (2011).
3. O. Lopez, A. Amy-Klein, M. Lours, C. Chardonnet, and G. Santarelli, Appl. Phys. B **98**, 723 (2010).
4. A. X. Zhang, Y. T. Dai, F. F. Yin, T. P. Ren, K. Xu, J. Q. Li, Y. F. Ji, T. Lin, and G. S. Tang, Opt. Lett. **38**, 2419 (2013).
5. M. Fujieda, M. Kumagai, T. Gotoh, and M. Hosokawa, IEEE Trans. Instrum. Meas. **58**, 1223 (2009).
6. B. Wang, C. Gao, W. L. Chen, J. Miao, X. Zhu, Y. Bai, J. W. Zhang, Y. Y. Feng, T. C. Li, and L. J. Wang, Sci. Rep. **2**, 556 (2012).
7. L. M. Zhang, L. Chang, Y. Dong, W. L. Xie, H. He, and W. S. Hu, Opt. Lett. **36**, 873 (2011).
8. B. Ning, D. Hou, T. L. Zheng, and J. Y. Zhao, IEEE Photon. Technol. Lett. **25**, 1551 (2013).
9. F. Narbonneau, M. Lours, S. Bize, A. Clairon, G. Santarelli, O. Lopez, C. Daussy, A. Amy-Klein, and C. Chardonnet, Rev. Sci. Instrum. **77**, 064701 (2006).
10. J. G. Shen, G. L. Wu, W. W. Zou, R. H. Chen, and J. P. Chen, Appl. Opt. **52**, 8332 (2013).
11. U. Gliese, S. Norskov, and T. N. Nielsen, IEEE Trans. Microwave Theor. Technol. **44**, 1716 (1996).
12. J. G. Shen, G. L. Wu, W. W. Zou, and J. P. Chen, Appl. Phys. Express **5**, 072502 (2012).
13. B. Hraimel, X. P. Zhang, Y. Q. Pei, K. Wu, T. J. Liu, T. F. Xie, and Q. H. Nie, J. Lightwave Technol. **29**, 775 (2011).
14. C. Gao, B. Wang, W. L. Chen, Y. Bai, J. Miao, X. Zhu, T. C. Li, and L. J. Wang, Opt. Lett. **37**, 4690 (2012).